

Total Cross Sections of Nuclei for 42-Mev Neutrons*

ROGER H. HILDEBRAND AND CECIL E. LEITH

Radiation Laboratory, Department of Physics, University of California, Berkeley, California

(Received July 24, 1950)

Total cross sections of 33 elements for 42-Mev neutrons have been measured using the 184-inch cyclotron as a source of neutrons and the $C^{12}(n,2n)C^{11}$ reaction as a detector. Experimental details are described and the results are compared with those measured at other energies.

I. INTRODUCTION

THE measurements of total neutron nuclear cross sections^{1,2} at 90 Mev showed effects interpretable in terms of nuclear transparency,³ whereas measurements at⁴ 14 Mev and at⁵ 25 Mev are interpretable in terms of an opaque nucleus.⁶ The $C^{12}(n,2n)C^{11}$ reaction as a neutron detector provides a simple method for measuring cross sections at an intermediate energy. The 40-Mev neutron beam intensity from the 184-inch cyclotron operated at reduced radius is sufficient to permit accurate cross-section measurements of a large number of elements in a relatively short time with the detector 15 meters from the source.

II. GENERAL FEATURES OF THE EXPERIMENT

The 42-Mev total cross sections were obtained by good geometry attenuation measurements using essentially the same method as was used by Cook, McMillan, Sewell and Peterson¹ at 90 Mev.

The neutron beam, produced by deuteron stripping in the cyclotron target strikes an attenuator (the material being investigated) about 5 meters from the target. The incident beam activates a monitor placed just outside of the cyclotron tank and the transmitted beam activates a detector which is placed about 10 meters beyond the attenuator (Fig. 1).

The fundamental measurement in this work is the ratio, r , of detector to monitor activity. This ratio

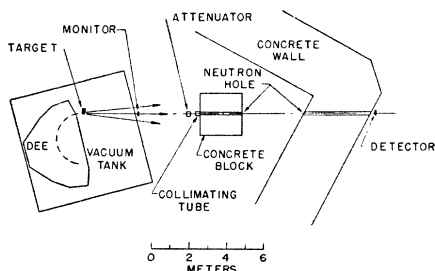


FIG. 1. Plan view of experimental arrangement.

* This work was performed under the auspices of the AEC.

¹ Cook, McMillan, Peterson, and Sewell, *Phys. Rev.* **75**, 7 (1949).

² DeJuren and Knable, *Phys. Rev.* **77**, 606 (1950).

³ Fernbach, Serber, and Taylor, *Phys. Rev.* **75**, 1352 (1949).

⁴ Amaldi, Bocciarelli, Cacciapuoti, and Trabacchi, *Nuovo Cimento* **3**, 203 (1946).

⁵ R. Sherr, *Phys. Rev.* **68**, 240 (1945).

⁶ H. Feshbach and V. F. Weisskopf, *Phys. Rev.* **76**, 1550 (1949).

should vary exponentially from some initial value r_0 to zero as the thickness of attenuator is varied from zero to infinity. A barely detectable background r_B persists, however, when an "infinite" attenuator consisting of 45 cm of copper is used. This amount of copper should transmit only about 10^{-4} of the incident flux which would be entirely beyond detection; hence the background must not be due to neutrons which have passed through the attenuator. Possible sources of this background are neutrons scattered by the vacuum tank wall and neutrons formed when the circulating cyclotron beam hits the dee. If, corresponding to attenuator thicknesses 0, x , and "infinity," we measure ratios of detector to monitor activity r_0 , r , and r_B the transmission T of a sample of thickness x is given by

$$T = (r - r_B) / (r_0 - r_B),$$

and the cross section is calculated from T using the relation,

$$\sigma = (-A/N\rho x) \ln T,$$

where $A/N\rho x$ = number of atoms per square centimeter.

III. NATURE OF SOURCE AND DETECTOR, MEAN DETECTION ENERGY

The neutron source is a 1.27 cm thick Be target bombarded by deuterons at a cyclotron radius of 55 in. where the magnetic field is 14.5 kilogauss. The neutron flux density from this target is of the order of 10^5 neutrons $\text{cm}^2 \text{sec}^{-1}$ at the detector.

The energy distribution of the neutron beam is calculated from the deuteron stripping theory of Serber⁷ taking into account the energy loss of the deuterons in the target. No experimental information exists on the energy distribution of the neutron beam at 40 Mev; however, measurements of both the angular distribution⁸ and the energy distribution⁹ at 90 Mev have demonstrated the validity of the stripping theory. This calculated neutron energy distribution is shown in Fig. 2 as curve A.

The neutrons were detected by measuring the activity they induced in carbon disks by the reaction $C^{12}(n,2n)C^{11}$. The manner in which the sensitivity of this detector varies with the neutron energy has not

⁷ R. Serber, *Phys. Rev.* **72**, 1008 (1947).

⁸ Helmholtz, McMillan, and Sewell, *Phys. Rev.* **72**, 1003 (1947).

⁹ Hadley *et al.*, *Phys. Rev.* **75**, 351 (1949).

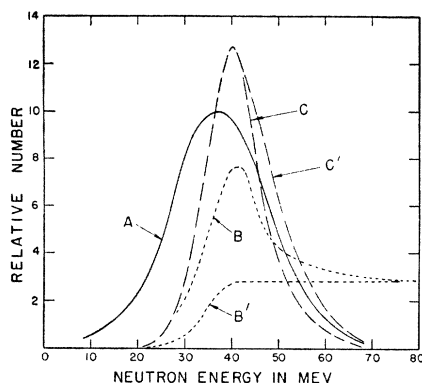


Fig. 2. Detection efficiency (see text).

been measured. The result of a theoretical calculation¹⁰ of this function is shown in Fig. 2 as curve *B*. The related theoretical calculation¹⁰ of the reaction $C^{12}(p,pn)C^{11}$ has been confirmed experimentally.^{11,12} A measurement of the $C^{12}(n,2n)C^{11}$ cross sections averaged over the 40-Mev and the 90-Mev neutron energy distributions have shown them to be approximately the same.¹³ Hence the peak in the theoretical curve *B* is probably too large with respect to the higher energy part of the curve whereas the arbitrary curve *B'*, which has the same shape as *B* to the left of the peak except for a scale factor, is probably too low in the 40-Mev region. The product curves $C = A \times B \times (\text{constant})$ and $C' = A \times B' \times (\text{constant})$ show the extent to which the expected energy distribution of the detected neutrons depends on the excitation function assumed. The constants have been adjusted to make *C* and *C'* coincide to the left of the peak. The mean detection energies corresponding to *C* and *C'* are 41.3 and 43.2 Mev. Since *B* and *B'* are believed to be limiting curves the true energy distribution of detected neutrons is assumed to lie between *C* and *C'* with a mean energy of about 42 Mev.

IV. APPARATUS AND EXPERIMENTAL PROCEDURE

The detectors were carbon disks 4.3 cm in diameter and 0.32 cm thick with a density of 1.59 ± 0.02 g/cm³. One such disk was used as a monitor of the incident beam and two were used as detectors of the transmitted beam. During bombardment the disks were placed in aluminum holders which were fixed in the positions indicated in Fig. 1. At the end of the run the (20 min.) β^+ -activity was counted on mica-window Geiger-Müller counters. The counts of the two detector disks were added. All counts were made concurrently; i.e., the detector and monitor activities were counted over the same time interval eliminating the necessity of corrections for decay.

A typical determination of r_0 (see Section II) in-

¹⁰ W. Heckrotte and P. Wolff, Phys. Rev. **73**, 264, 265 (1948).

¹¹ W. W. Chupp and E. M. McMillan, Phys. Rev. **72**, 873 (1947).

¹² E. M. McMillan and R. D. Miller, Phys. Rev. **73**, 80 (1948).

¹³ R. L. Mather and H. F. York, unpublished.

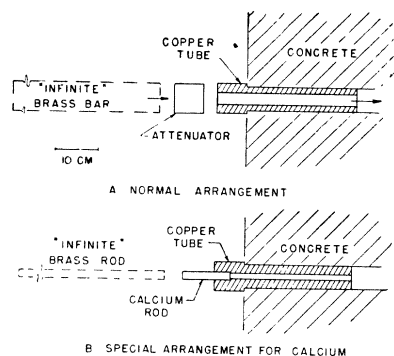


Fig. 3. Detail of collimating system and absorber.

involved about 20,000 net counts from the detector disks in a period of 15 minutes. This is about 100 times the counter background and about 3 times the net count in determining r for a typical attenuator. In determining r_B a typical detector count was 500 of which 460 were counter background.

A 2.5 cm i.d. copper collimating tube was placed just behind the attenuator as shown in Fig. 3. This was to prevent neutrons from reaching the detector unless they had passed through the attenuator. Because of the divergence of the beam, its diameter at the detector was about 7 cm hence the detectors could be placed entirely within the beam. The alignment of the apparatus was checked before each series of runs using x-ray films exposed in the beam. The equipment was adjusted so that the shadow of a small object in the attenuator position and the circular spot transmitted by the collimator were centered on the detector position.

The absence of spurious counts was demonstrated by the exponential nature of attenuation curves which were made (Fig. 4) and by the barely detectable background which was observed when the "infinite" attenuator was used.

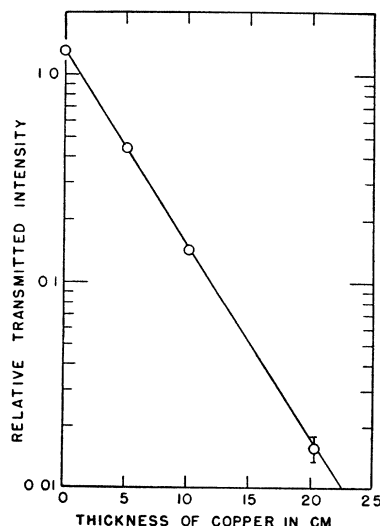


Fig. 4. Attenuation of 40-Mev neutrons in copper.

TABLE I. Cross sections of elements. (The errors shown are standard deviations calculated from the counting statistics alone.)

Element	Form ^a	σ_t in barns	Z Atomic number	M Atomic weight	$M^{\frac{1}{2}}$	$R = (\sigma_t/2\pi)^{\frac{1}{2}}$ in units of 10^{-12} cm
H	<i>d</i>	0.203±0.007	1	1.008	1.00	0.180±0.003
D	<i>d</i>	0.289±0.013	1	2.015	1.26	0.214±0.005
Li	<i>s</i>	0.684±0.011	3	6.940	1.91	0.330±0.003
Be	<i>s</i>	0.853±0.010	4	9.02	2.08	0.368±0.002
B	<i>p</i>	0.985±0.020	5	10.82	2.21	0.396±0.004
C	<i>d</i>	1.089±0.011	6	12.01	2.29	0.416±0.002
N	<i>d(p)</i>	1.220±0.025	7	14.008	2.41	0.441±0.005
O	<i>d</i>	1.358±0.012	8	16	2.52	0.465±0.002
F	<i>d(p)</i>	1.603±0.030	9	19.000	2.67	0.505±0.005
Na	<i>d(p)</i>	1.67 ±0.06	11	22.997	2.84	0.515±0.009
Mg	<i>s</i>	1.723±0.024	12	24.32	2.90	0.524±0.004
Al	<i>s</i>	1.782±0.020	13	26.97	3.00	0.532±0.003
S	<i>d</i>	1.974±0.030	16	32.06	3.18	0.560±0.004
Cl	<i>d</i>	2.11 ±0.04	17	35.457	3.29	0.579±0.005
Ca	<i>s</i>	2.210±0.026	20	40.08	3.42	0.592±0.004
Fe	<i>s</i>	2.441±0.021	26	55.85	3.82	0.623±0.003
Ni	<i>s</i>	2.510±0.034	28	58.69	3.88	0.632±0.004
Cu	<i>s</i>	2.540±0.019	29	63.57	3.99	0.636±0.003
Zn	<i>s</i>	2.618±0.027	30	65.38	4.03	0.646±0.003
Br	<i>d</i>	2.93 ±0.06	35	79.916	4.30	0.682±0.007
Sr	<i>d(p)</i>	2.99 ±0.12	38	87.63	4.44	0.690±0.014
Mo	<i>s</i>	3.11 ±0.05	42	95.95	4.58	0.703±0.006
Ag	<i>s</i>	3.229±0.034	47	107.880	4.76	0.716±0.004
Sn	<i>s</i>	3.251±0.023	50	118.70	4.91	0.719±0.003
I	<i>d</i>	3.51 ±0.06	53	126.92	5.03	0.747±0.006
Ba	<i>d(p)</i>	3.57 ±0.12	56	137.36	5.16	0.753±0.013
Ta	<i>s</i>	4.20 ±0.04	73	180.88	5.66	0.817±0.004
W	<i>s</i>	4.31 ±0.06	74	183.92	5.69	0.828±0.006
Hg	<i>l</i>	4.51 ±0.06	80	200.61	5.85	0.846±0.006
Pb	<i>s</i>	4.44 ±0.05	82	207.21	5.92	0.840±0.005
Bi	<i>s</i>	4.58 ±0.06	83	209.00	5.94	0.853±0.006
Th	<i>s</i>	5.03 ±0.07	90	232.12	6.14	0.894±0.006
U	<i>s</i>	5.12 ±0.07	92	238.07	6.20	0.902±0.006

^a *d* = derived from measurements listed in Table II; *s* = solid; *l* = liquid; *p* = powder; *d(p)* = derived from a powdered compound.

The substances which were used in the form of solid blocks were paraffin, Li, Be, C, Mg, Al, Ca, Fe, Ni, Cu, Zn, Mo, Ag, Sn, Ta, W, Pb, Bi, Th, U. In all cases except calcium (see below) the cross section of the attenuating block was much greater than the cross section of the collimator (2.54 cm diameter) just behind them, being 5 cm×7½ cm in most cases. The thickness of the attenuating blocks was made one to two mean free paths whenever this much material was available and was never less than half of a mean free path. In many cases the "blocks" were actually stacks of thin slabs placed normal to the beam. The Be, Sn, Pb, Bi, and Th were machined from castings while all the others except Li and Ca were machined from stock. Two samples each of Be, Sn, Pb, and Th were used to reduce the chance of error due to imperfect castings. In the case of Li, blocks which had previously been pressed in a die were accurately machined under liquid vaseline. Since calcium was available only in the form of a rough cathode rod of small cross section a special collimating system had to be used. The rod was machined to a diameter of 1.75 cm and a length of 16.5 cm and used as shown in Fig. 3.

The liquids used were Hg, O, CS₂, CCl₄, CH₂Br₂, CH₂I₂, H₂O, D₂O, and pentane. The Hg was contained

in a rectangular aluminum can with the same cross section as that of the solid blocks and a length of 11 cm. The liquid oxygen container was a stainless steel tank with a 13 cm×13 cm cross section and a length of 38 cm. This tank was surrounded by asbestos so that there was very little boiling and almost none in the region near the long axis of the tank through which the detected neutrons passed. The CS₂, CCl₄, CH₂Br₂, and CH₂I₂ were contained in glass tubes 3 cm in diameter and 14 cm in length. The ends of the glass tubes were ¼-in. plate glass and were made accurately parallel. The water, heavy water and pentane were contained in brass cylinders 34 cm long and 6½ cm in diameter. In each case the intensity corresponding to zero attenuator thickness was measured using the appropriate empty container.

The powdered substances used were B, melamine (C₃N₆H₆), S, LiF, NaCl, SrCO₃ and BaCO₃. These powders were put into 3.6 cm diameter brass tubes 20 to 30 cm long with 0.2 cm thick aluminum ends and were packed as uniformly as possible over the cross section of the tube. To minimize errors due to non-uniform packing the tubes were refilled and, of course, reweighed before each run. At least two runs were made in every case.

V. RESULTS

Cross sections of all the elements investigated are given in Table I. Those marked "*d*" are derived from the measurements shown in Table II by averaging all independent determinations for each element. For example, the carbon cross section in Table I is the weighted average of three independent determinations: (1) directly measured carbon; (2) the carbon disulfide-powdered sulfur difference; (3) the hydrocarbon-hydrogen difference, where the hydrogen used was that obtained from the water-liquid oxygen difference.

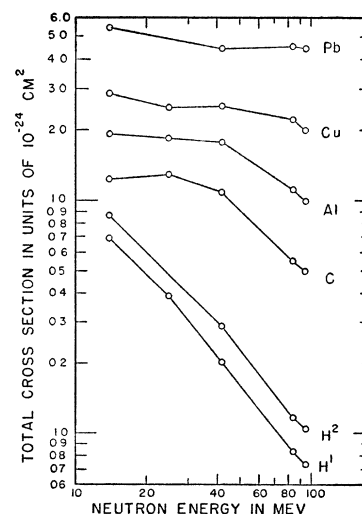


FIG. 5. Comparison of cross sections measured at various energies.

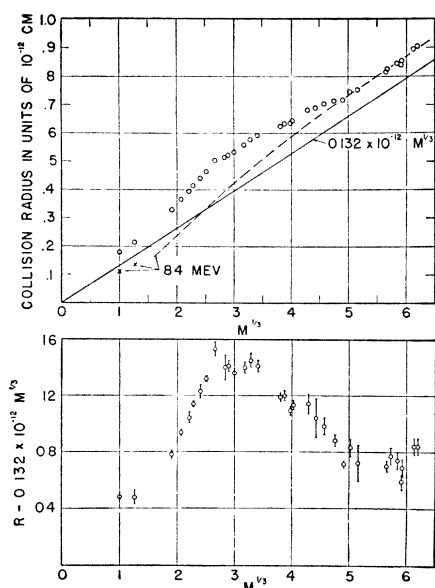


FIG. 6. Collision radii. The upper plot shows collision radii $R = (\sigma_t/2\pi)^{1/2}$ plotted against cube roots of atomic weights.

Collision radii measured by Cook *et al.* at 84 Mev are represented by the dashed curve with radii of H and D shown separately. The points shown in the lower plot are obtained by subtracting $0.132 \times 10^{-12} M^{1/3}$ from the collision radii.

Figure 5 shows a comparison of several of the 42-Mev total cross sections given in this paper with those measured at 14 Mev,⁴ 25 Mev,⁵ 84 Mev,¹ and 95 Mev.² In the paper of Cook *et al.*¹ the energy is given as “. . . between 80 and 90 Mev.” The figure 84 Mev given above is an estimate of the most probable value based on the references given in Section III. Additional measurements of hydrogen, deuterium and carbon have been made at energies below 25 Mev by several investigators.¹⁴⁻¹⁶

It is customary¹ to define a “collision radius” R by the expression

$$\sigma_t = 2\pi R^2,$$

where σ_t is the measured total cross section. This definition based on the assumption of an opaque nucleus provides an estimate of the nuclear radius. Figure 6 shows collision radii plotted against the cube roots of

¹⁴ W. Sleator, Jr., Phys. Rev. **72**, 207 (1947).

¹⁵ E. O. Salant and N. F. Ramsey, Phys. Rev. **57**, 1075 (1940).

¹⁶ Ageno, Amaldi, Bocchiarelli, and Trabacchi, Phys. Rev. **71**, 20 (1947).

TABLE II. Directly measured cross sections not listed in Table I. (The errors shown are standard deviations calculated from the counting statistics alone.)

Substance ^b	Form ^a	σ_t in barns
CH _{2.08} (paraffin)	<i>s</i>	1.510±0.031
CH _{2.4} (pentane)	<i>l</i>	1.568±0.018
H ₂ O	<i>l</i>	1.774±0.020
D ₂ O	<i>l</i>	1.935±0.023
N ₂ CH ₂ (melamine)	<i>p</i>	3.936±0.046
LiF	<i>p</i>	2.287±0.028
NaCl	<i>p</i>	3.777±0.045
C	<i>s</i>	1.092±0.011
S	<i>p</i>	1.985±0.036
CS ₂	<i>l</i>	4.989±0.105
CCl ₄	<i>l</i>	9.516±0.148
CH ₂ Br ₂	<i>l</i>	7.361±0.106
SrCO ₃	<i>p</i>	8.150±0.118
CH ₂ I ₂	<i>l</i>	8.523±0.109
BaCO ₃	<i>p</i>	8.731±0.109
O	<i>l</i>	1.353±0.014

^a *s* = solid; *l* = liquid; *p* = powder.

^b The cross sections refer to the formulas given, e.g., the “paraffin” cross section is that for one atom of C + 2.08 atoms of H.

the atomic weights. Collision radii obtained by Cook *et al.* at 84 Mev are represented by the dashed curve with radii of H^1 and H^2 shown separately. The points shown in the lower plot are obtained by subtracting $0.132 \times 10^{-12} M^{1/3}$ cm from the collision radii. This plot makes it possible to show the statistical errors associated with the points and shows the deviation of the points from a linear dependence on $M^{1/3}$.

An analysis of the consistency of individual measurements has been made for two groups of data: first, a group of 65 measurements involving solid and liquid attenuators; and second, a group of 23 measurements involving powdered attenuators. The first group showed a spread just consistent with the errors due to counting statistics (given in the tables). The second group showed random errors eight percent greater than those expected from counting statistics alone. The larger spread in the powder measurements is assumed to be due to the difficulty in obtaining uniform packing of the powder tubes. This apparent random error raises the question of possible non-random packing errors hence the powder measurements are probably less reliable than the others.

The authors wish to thank Professor E. O. Lawrence and Dr. B. J. Moyer for their interest in this work. We also wish to thank Mr. James Vale and the cyclotron operating crew for their assistance.